Astron. Astrophys. 353, 1074–1082 (2000)

ASTRONOMY AND ASTROPHYSICS

Magnetic reconnection in kinked coronal loops

H. Baty

Observatoire Astronomique, 11 Rue de l'Université, 67000 Strasbourg, France (baty@astro.u-strasbg.fr)

Received 6 August 1999 / Accepted 2 November 1999

Abstract. The resistive dissipation process triggered by the non linear development of the kink instability in a coronal loop is investigated using a three-dimensional MHD code in cylindrical geometry. An equilibrium flux tube carrying a zero net axial current is considered. The magnetic field lines are locally twisted in the central region and inertially anchored at the two photospheric end-plates. When the twist exceeds a critical value, the loop becomes kink unstable and an intense electric current concentration develops along the loop length (Baty et al. 1998). It is found that the system settles into a steady state where a magnetic reconnection of field lines consistent with the Sweet-Parker model occurs, in spite of the three dimensional character of the present process. In particular, the Ohmic dissipation rate scales as the square root of the resistivity. The reconnection can release more than 50 percent of the free magnetic energy stored in the initial equilibrium. Consequences for the coronal activity are presented.

Key words: methods: numerical – Sun: corona – Sun: magnetic fields

1. Introduction

Magnetic reconnection plays a crucial role in astrophysical plasma dynamics. This is particularly true for the solar corona. This localized process converts magnetic energy into thermal and kinetic energies of plasma flows, and allows a global change of the magnetic topology through an alteration of the field lines connectivity. They are clear observational evidences from x-ray pictures taken by the Yokhoh satellite that a reconnection process takes place during the solar flare phenomenon (Tsuneta et al. 1991), and that it provides a substantial heating of the solar corona (Tsuneta 1996, Yoshida and Tsuneta 1996).

The basic physics of the magnetic reconnection requires the presence of a thin region called an X-line where the magnetic field changes orientations. A plasma flow towards the X-line is also necessary to squeeze sideways the fluid and maintain a current sheet structure. In a weakly resistive plasma (like the solar corona), the resistive diffusion is important only in this thin internal region where large magnetic gradients are present. The external region can be then treated in ideal magnetohydrodynamic (MHD) framework. Even though a resistive reconnection is considered in this paper, a small hyper-resistivity term due to the anomalous electron viscosity could also lead to a similar process (Aydemir 1987). The reconnection is said to be spontaneous when the external flow arises spontaneously as a result of an instability, or to be driven when external boundary conditions on the flow and on the magnetic field are imposed in an open system.

Since the pioneering work on the reconnection phenomenon by Giovanelli (1947), numerous analytical and numerical results have been obtained in hot plasmas and more specifically in the solar corona context (Priest 1990, Priest 1997 and references therein). Depending on the geometry, the physical parameters, and the boundary conditions, many different regimes qualified as slow or fast have been then identified. However, most of these studies have been carried out in two dimensions, and the three dimensional (3D) reconnection process has been considered only very recently (Priest 1997).

The development of MHD instabilities in a coronal loop is one possible route for the 3D reconnection phenomenon (Einaudi et al. 1997, Lionello et al. 1998a, Arber et al. 1999). Indeed, line-tied loops having a sufficient amount of magnetic twist are known to be $m = 1$ kink unstable (m being the azimuthal mode number) (Raadu 1972, Hood & Priest 1979, Einaudi & Van Hoven 1983). Simulations of this ideal MHD instability in the non linear regime have shown that an intense current concentration is forming along the loop length (Baty & Heyvaerts 1996, Baty 1997, Velli et al. 1997, Baty et al. 1998). The interpretation of these current concentrations as current sheets (i.e. true current singularities) in the ideal MHD framework is still under debate (see our discussion in paragraph 4.1). However, a small finite resistivity triggers the reconnection of field lines in the vicinity of these current layers when sufficiently large magnetic field gradients are created (Einaudi et al. 1997, Lionello et al. 1998a, Arber et al. 1999). As a consequence, a significant amount of magnetic energy can be released.

While there is a consensus on the smallness of the coronal resistivity, its more precise value is somewhat unknown. The aim of the present paper is to determine the reconnection rate. More precisely, we investigate the scaling of the reconnection rate as a function of the plasma resistivity, extending the previously mentioned studies where a very limited number of resistivity values

has been employed. This scaling is important because it also determines the reconnection regime. A reconnection process is generally said to be fast if either the flux annihilation rate at the X-line or the Ohmic dissipation rate scales quasi independently of any positive power of the resistivity. According to this definition, the classical two dimensional (2D) Sweet-Parker model (Sweet 1958, Parker 1963) is slow because its rate scales as the square root of the resistivity. To do so, a localized twisted cylindrical tube is considered in order to model a coronal loop equilibrium that could result from the application of localized photospheric vortex flows (Mikic et al. 1990). We then carry out numerical computations of the resistive non linear evolution of this loop using the SCYL code (Baty & Heyvaerts 1996).

The paper is organized as follows. The classical two dimensional model of Sweet-Parker including the viscosity effect is reviewed in Sect. 2. The equilibrium configuration and the numerical model are presented in Sect. 3. The next section is devoted to the numerical results. Finally, the consequences for the coronal activity are discussed and the conclusions are drawn.

2. The reconnection theory: the Sweet-Parker model

The basic features of the 2D Sweet-Parker (SP) reconnection process can be seen in Fig. 1. For simplicity, we consider a case where the magnetic field component perpendicular to the plane of the diagram is vanishing. The plasma is supposed to be squeezed from both sides into the X-point where $B = 0$. In our case, this plasma flow V_x is fed by the non linear development of the ideal kink instability. A discontinuity in the magnetic field is then forming, as one can see in Fig. 1b. The presence of a small resistivity η is important only in a thin region defining the reconnection region (shaded area in Fig. 1a) with a size of $2\delta * 2\Delta$, where δ is the thickness and Δ the width. The SP model assumes a stationary process where the magnetic flux convected towards the reconnection layer is mainly transformed into kinetic energy through a local resistive diffusion process. Consequently, a plasma flow V_y is driven in the direction perpendicular to the initial flow. The magnetic field discontinuity given by $2B_*$ is also supposed to be constant and independent of the resistivity during all the process.

2.1. The Sweet-Parker scaling

In the steady state, the rate of change in the magnetic flux of the external region must be equal to the flux annihilation rate at the X-point:

$$V_x B_* = \eta J, \tag{1}$$

where J is the amplitude of the current density at the X-point $J = B_*/\delta$, which is directed perpendicular to the (x, y) plane. Note that the vacuum magnetic permeability μ_0 is set to one in our units. The resistive effect is neglected outside the reconnection layer (the advection being dominant) contrary to the internal region where the resistive diffusion is dominant. Moreover, the conservation of mass gives,

$$V_x \Delta = V_y \delta, \tag{2}$$

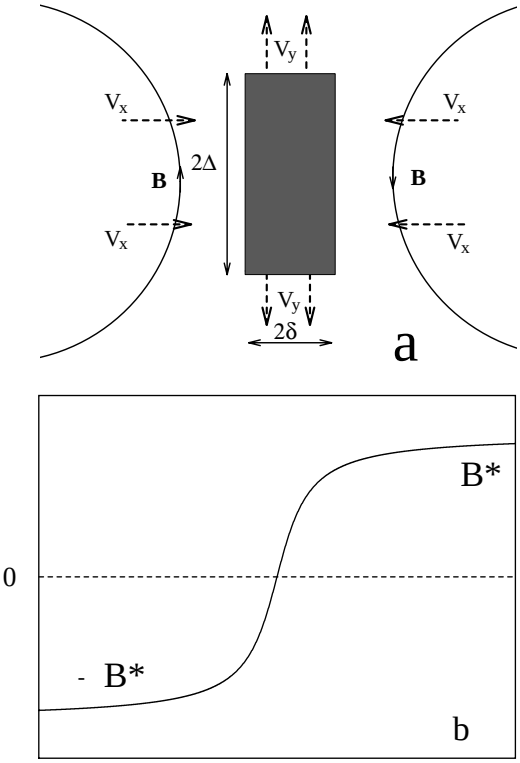

Fig. 1a and b. Schematic representation of the reconnection process. Intense gradients in the magnetic field are formed by compression due to plasma flow in the x direction **b**. The reconnection layer (shaded area) where diffusive effect is dominant represents a two dimensional region of extent $2\delta * 2\Delta$ **a**.

where we have supposed an incompressible plasma with equal densities inside and outside. Using Eqs. (1) and (2), one easily obtains:

$$\delta^2/\Delta = \eta/V_y. \tag{3}$$

The outflow velocity V_y is determined by the forces balance across and along the sheet. Neglecting the inertia term, one can find (Biskamp, 1993):

$$B_*^2/2 = \rho \frac{V_y^2}{2} + \rho\nu \frac{V_y/2}{\delta^2}\Delta, \tag{4}$$

where a viscous term is added to the acceleration term along the sheet. ν is the kinematic plasma viscosity corresponding to the ion viscosity, and ρ is the plasma density. The same equation can be also obtained writing that the work done by the pressure gradient in the y direction is balanced by the kinetic energy increase and the viscous dissipation (Park et al. 1984).

In the SP model, one assumes that Δ is independent of the resistivity and imposed by the geometry. We then obtain the following scaling for the thickness:

$$\delta = \rho^{1/4}\Delta^{1/2}B_*^{-1/2}\eta^{1/2}[1 + \frac{\nu}{\eta}]^{1/4}. \tag{5}$$

We also obtain the following scalings for the amplitude of the current density and the outflow velocity:

$$J = \rho^{-1/4}\Delta^{-1/2}B_*^{3/2}\eta^{-1/2}[1 + \frac{\nu}{\eta}]^{-1/4}, \tag{6}$$

$$V_y = \rho^{-1/2} B_* [1 + \frac{\nu}{\eta}]^{-1/2}. \quad (7)$$

The flux annihilation rate at the X-point defined by $\dot{\psi} = \eta J$ and the Ohmic dissipation rate in the layer given by $W = \eta J^2 \delta\Delta$ are then related to the resistivity by:

$$\dot{\psi} = \rho^{-1/4} \Delta^{-1/2} B_*^{3/2} \eta^{1/2} [1 + \frac{\nu}{\eta}]^{-1/4} \quad (8)$$

$$W = \rho^{-1/4} \Delta^{1/2} B_*^{5/2} \eta^{1/2} [1 + \frac{\nu}{\eta}]^{-1/4} \quad (9)$$

These scalings show the well known SP dependency on the resitivity of $\eta^{1/2}$ for either the annihilation rate at the X-point or the ohmic dissipation rate, when the viscosity term is set to zero. However, the viscosity is not zero in numerical simulations and one has to take it into account in order to correctly interpret the results. Note also that keeping a constant ratio ν/η when varying the resistivity gives the same scaling.

2.2. The Sweet-Parker model in cylindrical geometry

A reconnection process in agreement with the SP model is known to arise as a consequence of the non linear evolution of the internal kink mode in a cylindrical tokamak (Kadomtsev 1975). Indeed, it has been shown that a two dimensional process leading to the reconnection of magnetic surfaces is at work in this axially periodic configuration (Park et al. 1984, Baty et al. 1991). One has to consider the x direction as the radial one, and the y direction as an helical one directed along the $\boldsymbol{k}$ vector of the mode. The component B_* is then given by the projection of the equilibrium magnetic field on $\boldsymbol{k}$. The current density component corresponding to J is exactly helical along the cylinder directed along $\boldsymbol{B}$, and it is also radially located at the resonant surface where $\boldsymbol{k} \cdot \boldsymbol{B} = 0$ ($\boldsymbol{B}$ being the equilibrium magnetic field). A magnetic island is growing in the plasma core, and the reconnection stops when the system has reached a stable state of lower magnetic energy.

2.3. Other reconnection models

Contrary to the SP model where Δ is imposed by the system geometry and independent of the resistivity, the Petschek model (1964) that is again a steady state process assumes a reconnection region with $\Delta \simeq \delta$ independent of the resistivity. This has been initially introduced because it gives a fast process with a scaling for $\dot{\psi}$ independent of the resistivity. However, it has been recently obtained that Petschek's theory that is based on standing shock waves is incorrect in the limit of small resistivity (see discussion in Biskamp 1993). More recently, many dynamic models with a wide range of regimes have been derived (Priest 1997 and references therein). One can take, as an example of fast process, the flux pile-up regime of Biskamp and Welter (Biskamp & Welter 1980) occuring during the nonlinear development of the coalescence instability (Rickard & Craig 1993). A scaling independent of the resistivity has been obtained for the flux annihilation rate, while the Ohmic dissipation rate scales as $\eta^{-1/3}$.

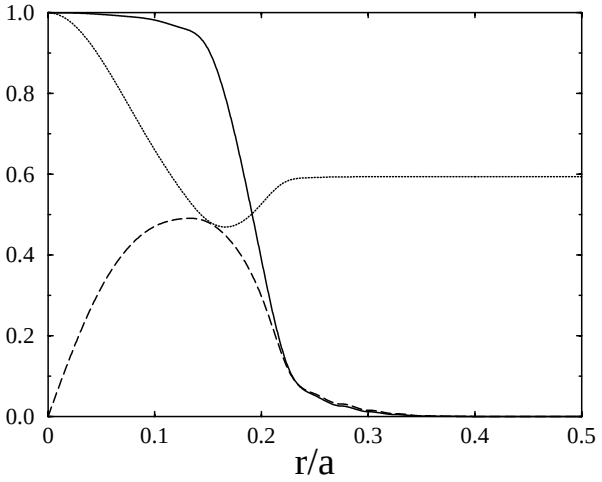

Fig. 2. The twist profile $\Phi(r)$ (plain line) and the corresponding azimuthal B_ϕ (dashed line) and axial B_z (dotted line) components of the equilibrium magnetic field. The magnetic field and twist values are normalized to their values on the magnetic axis.

3. The loop model and numerical procedure

3.1. The loop model

As in previous works on the kink instability in coronal loop, we neglect the toroidicity of the loop and model it by a cylindrical flux tube of length L. The footpoints of magnetic field lines are embedded in the dense photosphere at $z = \pm L/2$. A perfectly conducting wall is placed at the radial boundary $r = a$, sufficiently far enough from the axis in order to have a negligible influence on the loop dynamics (Mikic 1990, Lionello et al. 1998a).

As the corona is a low beta plasma, the plasma pressure is set to zero. We consider an axisymmetric force-free equilibrium defined by the twist profile:

$$\Phi(r) = \frac{L B_\theta}{r B_z}, \quad (10)$$

where B_θ and B_z are the azimuthal and axial components of the equilibrium magnetic field. Such 1D equilibrium approximates loop configurations resulting from imposed localized vortex flow at the photosphere and acting on a potential region (Mikic 1990). The radial variations of the equilibrium quantities assumed in the present study are plotted in Fig. 2. The internal region with a localized twist is surrounded by a potential region situated between $r/a = 0.4$ and $r/a = 1$ with a constant axial field and a vanishing azimuthal component. Contrary to previous studies (Lionello et al. 1998a, Arber et al. 1999) where the equilibrium is defined by analytic expressions of the magnetic field or current density components, the different profiles plotted in Fig. 2 are calculated numerically solving the radial force-free equilibrium equation. Note that, the total current flowing in the loop is zero. The twist value on the axis chosen in the present work is slightly higher than the critical twist value necessary to drive the kink instability unstable.

3.2. The numerical procedure

The evolution of the unstable loop configuration has been followed using the usual full set of compressible and diffusive MHD equations, written in the following dimensionless form:

$$\frac{\partial \rho}{\partial t} + \nabla \cdot (\rho \boldsymbol{v}) = 0, \tag{11}$$

$$\rho[\frac{\partial \boldsymbol{v}}{\partial t} + \boldsymbol{v} \cdot \nabla \boldsymbol{v}] = \boldsymbol{J} \times \boldsymbol{B} - \nabla P + \rho \nu \triangle \boldsymbol{v}, \tag{12}$$

$$\frac{\partial P}{\partial t} + \boldsymbol{v} \cdot \nabla p = -\gamma P \nabla \cdot \boldsymbol{v} \tag{13}$$

$$\frac{\partial \boldsymbol{B}}{\partial t} = \nabla \times (\boldsymbol{v} \times \boldsymbol{B}) - \nabla \times (\eta \boldsymbol{J}), \tag{14}$$

$$\boldsymbol{J} = \nabla \times \boldsymbol{B}. \tag{15}$$

Here, ρ is the mass density, P the plasma pressure, $\boldsymbol{v}$ the fluid velocity, $\boldsymbol{B}$ the magnetic field, $\boldsymbol{J}$ the electric current density. η and ν are the resistivity and the kinematic viscosity respectively, and γ is the ratio of specific heats (a value 5/3 is used). The energy equation is as simplified as possible, describing only energy convection (Eq. 13) because the aim of the present simulation is to understand primarily the dynamics. It would be easy to modify Eq. (13) to include Joule and viscous dissipation, and we plan to do so in future work.

The MHD equations (11–15) are integrated in time using a second order semi-implicit scheme, which allows large time steps only limited by the non linear physical plasma phenomena (Lerbinger & Luciani 1991).

Numerical computations are carried out using our code SCYL (Baty & Heyvaerts 1996, Baty 1997). The line-tying boundary conditions are modeled by imposing all the velocity components and also the perturbed magnetic field components to vanish at the photosphere. Radially, finite differences on two staggered meshes are used with 100 grid points. The radial mesh is also accumulated in regions where one expects large magnetic gradients to develop, the minimum resolution being $\Delta r = 0.004a$ at $r = 0.25a$. Fourier techniques are used in the $\theta * z$ directions giving 7 azimuthal modes ($m = 0, 1, ..., 7$), each with a band of 80 axial harmonics centered around the fastest growing one (Einaudi & Van Hoven 1983, Baty et al. 1998).

The simulations are initiated by adding an arbitrary small $m = 1$ velocity perturbation of amplitude $v \simeq 10^{-4}$ to the initial equilibrium considered. The initial plasma density is taken to be uniform and equal to unity in our dimensionless units. The twist value on the axis chosen in our study is $\Phi = 6.1\pi$, exceeding the critical twist of 5.6π that has been calculated using a linear version of our code (Baty & Heyvaerts 1996). The numerical aspect ratio of the loop is $L/a = 2.67$. Therefore, this unstable equilibrium is close to marginal stability but should have a sufficient linear growth rate to carry out reasonable computations without excessive waste of cpu time. We have artificially separated the non linear evolution into two different stages. Indeed, after a first stage where the resistivity coefficient η is set to zero in order to follow the formation of current concentrations, different resistivity values have been employed to simulate the ensuing reconnection process. The resistivity has been turned on at $t = T_r$ when the smallest magnetic scale approaches the grid resolution. A uniform resistivity is then introduced and maintained during all the second stage of the simulations. In principle, a non uniform resistivity localized in the regions of large magnetic gradients (or coupled to the current) should provide a more realistic result when the resistivity coefficient used is high (mainly for computational requirements). Indeed, a non uniform resistivity with a very small value outside the current layers avoids the diffusion of the whole equilibrium configuration. Conversely, a large uniform resistivity over all the computational domain overestimates the Ohmic heating while underestimating the kinetic energy (Arber et al. 1999). However, this result has been obtained for a dimensionless resistivity coefficient of order 10^{-3} in our units (the normalisation used here is that $a = 1$). Fortunately, we have been able to use lower resistivity values in the range [10^{-3}: 10^{-5}], the minimum value of 10^{-5} being limited by the residual numerical dissipation. Note also that a constant and uniform viscosity is used during this second stage, and that in most simulations the ratio of ν/η is kept constant and equal to 1.

4. Numerical results

4.1. Ideal phase

During the linear phase, the growth of the $m = 1$ kink mode is characterized by a linear growth rate $\gamma \simeq 0.35\, t_a^{-1}$, where $t_a = a/V_a$ is the Alfvén time and V_a is the Alfvén velocity on axis. By examining the radial components of the linear displacement and of the perturbed magnetic field, it has been obtained that the mode is well confined inside the current channel region of the equilibrium. This agrees with previous results showing that equilibria with a zero net current are subject to a so-called internal kink mode (Lionello et al. 1998a). Moreover, we have also obtained that the radial magnetic field perturbation (in the current region) only vanishes at a given radius $r = 0.2a$, at the loop apex (i.e. $z = 0$). This result is consistent with the presence of a resonant kink mode in our equilibrium (Velli et al. 1990).

When pursuing the simulation, the expected magnetic field gradients have been observed to develop. Indeed, an intense current concentration with an helical-like structure wrapping along the central loop region is forming. This current concentration appears as a negative peak superposed on the initial current density, and is radially localized at the previously mentioned resonance at the loop apex (Baty & Heyvaerts 1996). As time goes on, no saturation of the current peak has been observed for the magnetic equilibrium considered in the present study, even when a maximum viscosity coefficient of $\nu \simeq 10^{-3}$ is employed. In the same time, a magnetic length scale of diminishing thickness is also forming, reaching finally the grid scale.

This seems to contradict previous results where a saturated state with an intense but finite maximum current density (and minimum radial layer thickness) has been obtained (Baty 1997, Baty et al. 1998). Conversely, the present results agrees with

recent simulations obtained with a Lagrangian code (Arber et al. 1999), leading the authors to claim that current sheets (i.e. genuine singularities) are probably forming in this ideal MHD framework. This controversial point has been also noted when comparing with simulations obtained by Lionello et al. (1998a), leading to an explanation in terms of different treatment of small scales in the two codes (Baty et al. 1998). However, another possible interpretation can be given. Indeed, when it saturates, the maximum current peak has been observed to scale linearly or exponentially with the magnetic shear of the initial equilibrium profile (Baty 1997, Baty et al. 1998). The magnetic shear can be defined as $s = r\Phi^{'}/\Phi$, where $\Phi^{'}$ is the radial derivative of the twist. By Looking at the different shear profiles used in the simulations, a maximum value of order 15 has been employed by Arber et al. (1999) while smaller values in the range $[1:5]$ have been used in Baty et al. (1998). In the present case, a rather high maximum shear value of 10 can be deduced from Fig. 2. It is therefore possible that in simulations with high shear values, a saturation could occur but the resolution is not sufficient to observe it. Similar arguments have been proposed to explain the form of ideal current layers due to the non linear development of the line-tied coalescence instability (Longcope & Strauss 1993).

Since Parker's model of coronal heating (1972), the existence of true current singularities in ideal MHD framework is still actually highly controversial (Ng & Bathachargee 1998 and references therein). However, the crucial question is: the solar corona resistivity being given, can the current concentrations be large enough to trigger a reconnection process? According to the previous discussion, at least for some equilibria the answer is affirmative.

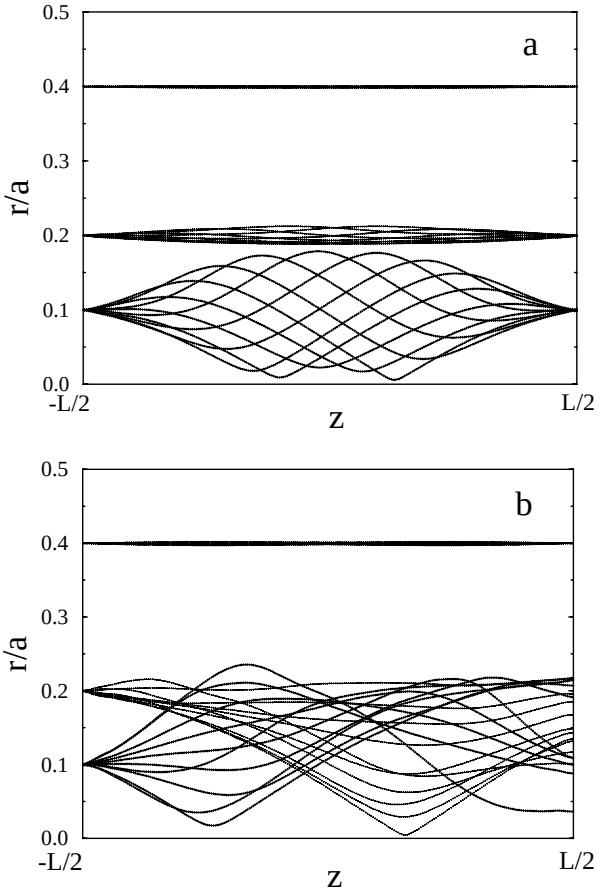

Fig. 3a and b. Mapping of three sets of ten field lines originating from $r/a = 0.1, 0.2$, and 0.4 at $z = -L/2$, projected into the (r, z) plane, at the end of the ideal phase **a** and at a given time during the resistive phase **b**.

4.2. Evidence for a stationary reconnection process

As already explained in this paper, the second phase of the simulation is followed by allowing a non vanishing value for the resistivity coefficient η in Equ. 14. Therefore, the resistivity is introduced after a time $T_r \simeq 23.7\, t_a$ determined by the current state that gives a critical value of $2J_{equ}$ for the maximum amplitude of the current density concentration (J_{equ} is the maximum equilibrium current density). A similar procedure has been also used by Arber et al. (1999).

In a periodic loop like a cylindrical tokamak, the magnetic reconnection associated with the internal kink instability is a two dimensional process where helical symmetry is preserved. This means that the helical flux is the appropriate quantity to examine (Baty et al. 1991). In a line-tied loop, the magnetic surfaces concept is not well defined, and the three dimensional character lead to the necessity to examine the mapping of the field lines from one photospheric end to the other (Lionello et al. 1998b). Therefore, three sets of 10 field lines originating from three radius situated at one photospheric plane at $z = -L/2$ have been selected. For each set, the 10 field lines are also rooted at 10 equidistant azimuthal positions at $z = -L/2$. After integration along the loop length, these field lines are connected to the other photospheric plane situated at $z = L/2$. Such mapping projected into the (r, z) plane has been plotted in Fig. 3 for two times, at the end of the ideal phase and for a given time $t = 28.71\, t_a$ during the second resistive phase (with $\nu = \eta = 5.62\, 10^{-5}$). Fig. 3a shows that the lines are not confined to their initial radius due to the deformation induced by the development of the ideal kink instability. As an example, internal lines originating from $r/a = 0.1$ at $z = -L/2$ experiment a radial excursion until $r/a = 0.17$ at the loop apex. This maximum excursion is smaller for the more external lines originating from radius situated at $r/a = 0.2$ and negligible for the lines at $r/a = 0.4$. At $z = L/2$, all these lines are finally connected to their original radii, as the connectivity cannot change in ideal MHD. This is not the case during the resistive phase (Fig. 3b) where a change of lines connectivity has been observed, meaning that a reconnection process is at work. Indeed, the lines originating from $r/a = 0.1$ at $z = -L/2$ can be now connected to different radii at $z = L/2$. Note that symmetric lines originating from a given radius at $z = L/2$ could be also obtained, but are not plotted in Fig. 3b to facilitate the visualization.

We have followed in details the time evolution of different given field lines that can be identified by their original radii and azimuthal positions at $z = -L/2$. We have obtained that a field line experiments different reconnecting events when its

trajectory intersects the current concentration region. The results will be reported in a forthcoming paper.

In order to investigate the time evolution of the system, we have first examined the magnetic energy (integrated over all the computational domain) contained in the azimuthal component of the magnetic field. This quantity is the adequate one to measure the main part of the non potential energy that is available to be released. Even though we consider a global quantity, the main contribution in the energy to be dissipated comes from the current concentration region. The results are plotted in Fig. 4 for three cases $\eta = \nu = \sqrt{10}.\,10^{-4}, 10^{-4}$, and $\sqrt{10}.\,10^{-5}$. After the ideal phase characterized by a quasi-constant value and a very short transition near T_r, a stationary regime with an exponentially decreasing variation is established. We can confirm this result by inspecting the time evolution of local parameters which define the resistive current layer, measured at the loop apex for commodity. These parameters are the amplitude of the current density (called J in Sect. 2.1), and the maximum azimuthal velocity which gives an estimate of the outflow velocity V_y. The results for $\eta = \nu = 10^{-4}$ are plotted in Fig. 5, showing that a steady state with constant values is rapidly established. Similar results have been also obtained for other values of the dissipation coefficients, except when the resistivity is high ($\eta \sim 10^{-3}$). Indeed, as previously discussed in this paper, a rather high value of the resistivity leads to the unrealistic diffusion of the whole equilibrium.

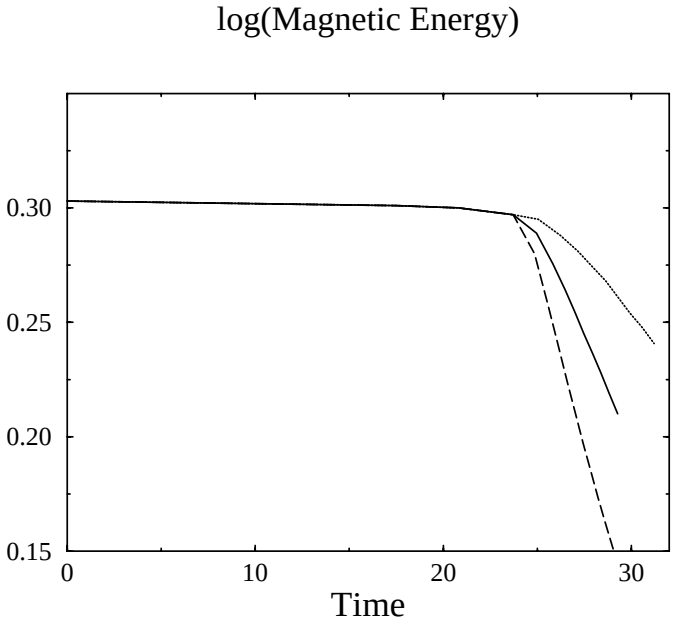

Fig. 4. Time evolution of the azimuthal magnetic energy for three dissipation coefficient values, $\eta = \nu = \sqrt{10}.\,10^{-4}$ (dashed line), 10^{-4} (plain line), and $\sqrt{10}.\,10^{-5}$ (dotted line).

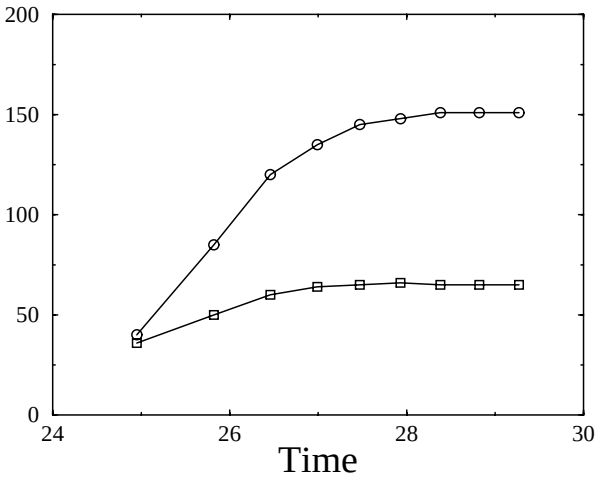

Fig. 5. Resistive time evolution (for $\eta = \nu = 10^{-4}$) of maximum values of current density amplitude (square) and azimuthal velocity (circle), measured at the loop apex. The values are reported in arbitrary units in order to be plotted on the same graph.

4.3. Scaling of the reconnection process with resistivity

Once a steady state is established, the rate at which the reconnection proceeds is determined by the form of the current concentration region. We have obtained that the current concentration takes the form of a quasi-helical ribbon wrapping along the central region and extending along the loop length, in agreement with previous works (see Fig. 7 in Arber et al. 1999). We have plotted in Fig. 6 the parallel component of the current density defined as $\alpha = \boldsymbol{j} \cdot \boldsymbol{B}/B^2$, for a given azimuthal direction at the loop apex that corresponds to the maximum in current amplitude. One can easily see the peak that characterizes this current layer. The amplitude of this peak is not constant along the loop length, but is maximum at the loop apex and minimum at the photosphere (Fig. 7).

In order to determine the rate at which the reconnection proceeds, we have first investigated the dependence of the maximum in α measured at the loop apex as a function of the resistivity coefficient η (9 values have been used). The results that are reported in Fig. 8a, follow a SP scaling law in $\eta^{-1/2}$ for η values smaller than $\sim 3.\,10^{-4}$. For higher η values, another regime probably due to a whole diffusion process is effective. The results for the azimuthal velocity are reported in Fig. 8b, showing that a constant value of $0.15V_a$ independent of the resistivity is obtained for intermediate η values that are in the range $[3.10^{-4} : 3.10^{-5}]$. We recall that a constant value for the outflow velocity V_y is also predicted by a SP mechanism. As expected, the outflow velocity values are smaller when the resistivity is higher (Arber et al. 1999). However, velocity values smaller by a few percent have been also obtained when the resistivity is lower than $3.\,10^{-5}$. Indeed, when $\eta \simeq 10^{-5}$, we have observed oscillations in time of the velocity making precise values difficult to measure. These oscillations are probably due to numerical effects. Indeed, in this case, very large gradients that are only marginally resolved are obtained. Another possible explanation can be also given in terms of bursty reconnection. Indeed, numerical simulations by Galsgaard & Nordlund (1996, 1997) have suggested such effect where the initial current sheet breaks into a hierarchy of secondary sheets that dissipate on different time and length scales. We have finally measured the time scale of the exponential decay of the non potential energy

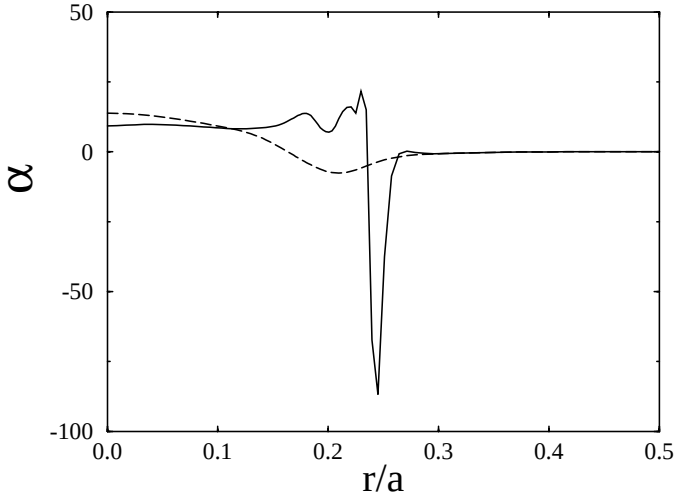

Fig. 6. The radial variation of α at the loop apex is plotted for $\nu = \eta = 5.62\,10^{-5}$ (plain line). It is obtained for a particular θ value corresponding to the direction of the maximum current peak amplitude. The same quantity corresponding to the initial equilibrium configuration is also plotted in dashed line

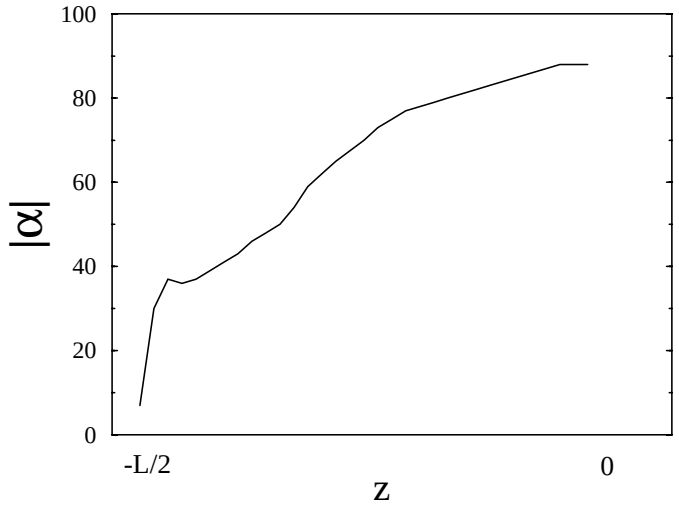

Fig. 7. The maximum value of α is plotted as a function of the axial coordinate z, obtained for $\nu = \eta = 5.62\,10^{-5}$.

(see Fig. 4) in order to determine a characteristic time scale τ for the process. As one can see in Fig. 8c, the resulting scaling in $\eta^{-1/2}$ agrees again very well with rates predicted by the SP model as long as η is not too high (i.e. $\eta \leq 3.\,10^{-4}$).

4.4. Viscosity effect

Finally, we have superficially investigated the effect of the viscosity by keeping a constant resistivity coefficient $\eta = 10^{-4}$. Three viscosity values $\nu = 10^{-5}, 10^{-4}, 10^{-3}$ have been then used. Numerically, we find $\alpha(10^{-5})/\alpha(10^{-4}) = 1.076$ and $\alpha(10^{-5})/\alpha(10^{-3}) = 1.89$, while Eq. (6) gives theoretical values of 1.16 and 1.78 respectively. The numerical outflow velocity ratios are $v(10^{-5})/v(10^{-4}) = 2$ and $v(10^{-5})/v(10^{-3}) = 3.75$, while Eq. (7) gives SP values of 1.35 and 3.16. The observed values are then only in rough agreement with the SP model.

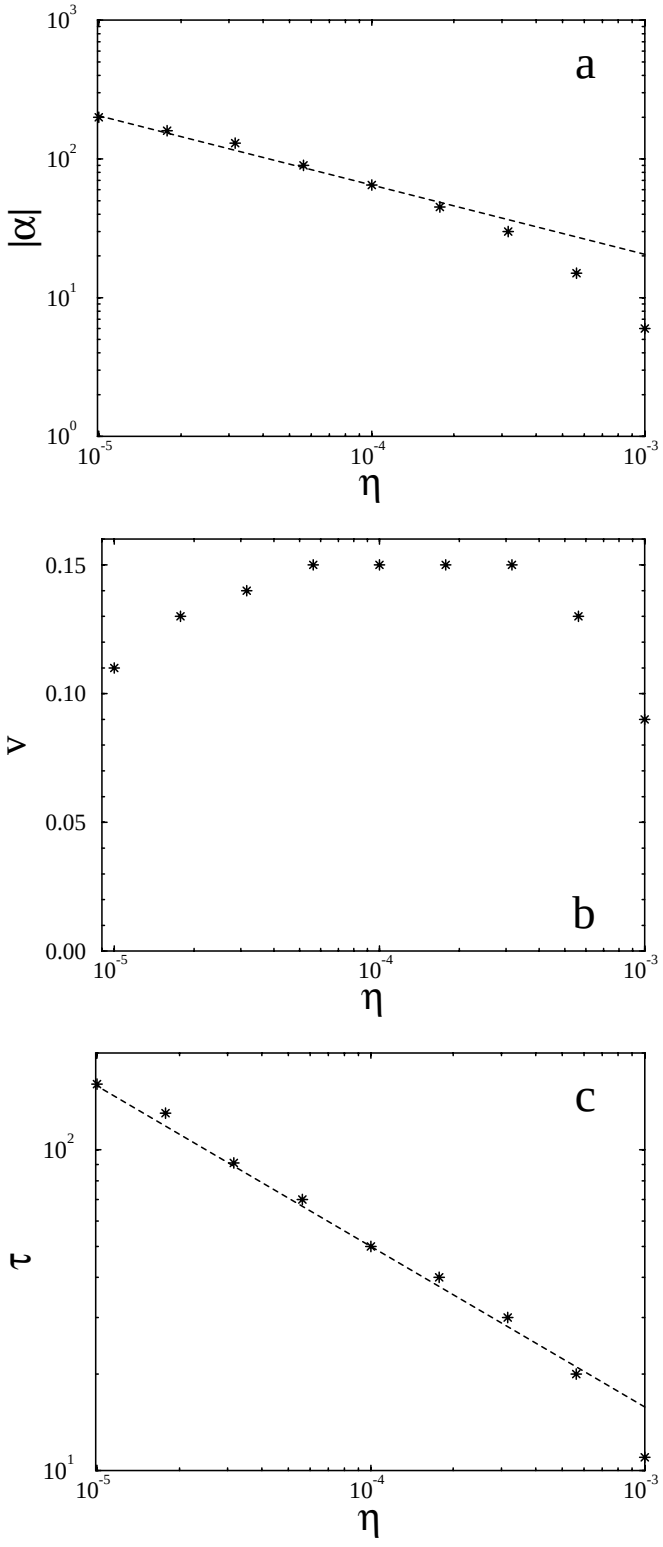

Fig. 8a–c Scaling of maximum α **a**, maximum azimuthal velocity **b**, and characteristic time scale τ **c**, as a function of the resistivity η. Theoretical SP scaling in $\eta^{-1/2}$ is indicated by the dashed line.

4.5. Final state

We have completed the time evolution of the system until a final relaxed state of lower magnetic energy was obtained. This has been done for only one value of the dissipation coefficient, that is $\eta = \nu = 3.33\,10^{-4}$. These values are optimal ones as higher values lead to a somewhat important diffusion of the whole configuration while smaller values lead to a considerable time of CPU computation.

The final state that has been obtained in the present study is characterized by internal field lines having a very small amount of twist compared to the initial magnetic configuration, while the external field lines in the potential region are not affected. This result is consistent with previous studies (Einaudi et al. 1997), and was expected as the kink mode is driven unstable because a critical twist is exceeded. Moreover, it is found that 57 percent of the free magnetic energy contained in the non potential magnetic field is released, that is in good agreement with the value of 54 percent obtained by Arber et al. (1999) for a similar unstable equilibrium.

5. Discussion and conclusion

In this study, we have presented a numerical study of the resistive magnetic reconnection process that occurs during the non linear evolution of MHD kink instabilities in coronal loops. We have concentrated on a single equilibrium configuration carrying no net current in the cylindrical geometry approximation, and having twisted magnetic field lines in the central region.

First, the formation of a quasi-helical current concentration extending all along the loop length has been obtained, in agreement with previous studies. As time goes on, no saturation of the amplitude of the current concentration has been observed in the limit of vanishing resistivity. This confirms recent results for a similar equilibrium (Arber et al. 1999), even though saturated secondary bifurcated equilibria containing a current layer of finite amplitude with a non vanishing thickness have been also obtained for other equilibria (Baty et al. 1998). This apparent lack of consensus could be explained by the use of different equilibrium parameters and/or different numerical procedure, and it is beyond the scope of the present paper.

Second, we have explored the resistive dissipation mechanism that takes place when a non zero resistivity value is allowed. Different resistivity coefficients ranging from 10^{-3} to 10^{-5} in our dimensionless units have been arbitrarily introduced when the smallest magnetic scale generated is approaching the grid scale. A magnetic reconnection has been then observed to occur through a change of field lines connectivity. In spite of its three dimensional character, the present process is consistent with the 2D stationary model of Sweet-Parker. Indeed, we have obtained that the rates of both the Ohmic dissipation and the flux annihilation at the X-line scale as $\eta^{1/2}$. This means that the available magnetic energy driving the configuration unstable is released almost equally in Ohmic heating and kinetic energy, as long as the viscous effect is neglected. Note that this is consistent with Arber et al.'s conclusion (1999), even though no scaling study has been made in this latter study.

Note that, when investigating such scaling with the resistivity by means of numerical computations, one has to take care about two important points. First, when varying η, the ratio of the viscosity coefficient to resistivity one must be kept constant (see Eqs. 8–9). One can also consider the $\nu/\eta << 1$ regime, ν being determined by the residual numerical viscosity. However, in this latter case, we have obtained that oscillations in velocity prevent us from measuring precise values of the relevant parameters. Second, the use of an uniform viscosity in all the computational domain is valid as long as the resistivity value is not too high (η must be lower than $\sim 3.\,10^{-4}$ in our dimensionless units). This is in agreement with the conclusion obtained by Arber et al. (1999).

The process has been observed to stop when a relaxed state of lower magnetic energy is reached. The energy released during the reconnection is 57 percent of the available energy that was stored in the azimuthal component of the equilibrium field, and 12 percent of the total amount of magnetic energy of the loop configuration. The final state is characterized by field lines having a lower amount of twist than for the initial configuration.

Numerical simulations always require the use of a minimum resistivity which is larger than the coronal value. Even though we have been able to consider rather low η values of order 10^{-5} in this study, the coronal resistivity is thought to be of order 10^{-13} in our units. In presence of current driven micro-instabilities (Rosner et al. 1978, Beaufumé et al. 1992), an anomalous resistivity enhanced by several orders of magnitude over the classical value can be also obtained. Assuming that the Sweet-Parker scaling remains valid for a range of smaller η values relevant for the solar corona, we can extrapolate our results to real coronal values. First, as discussed in Sect. 4.1, we must consider kinked loops generating current concentrations that would continue to collapse to smaller and smaller scales until the resistive dissipation triggers the reconnection process. As we have obtained that the resistive phase takes about 7 Alfvén times for $\eta = 3.33\,10^{-4}$. It corresponds to 7s when one assume typical values in active regions of 100G for the magnetic field strength, 10^8m for the loop radius a, and 10^{-12} kg/m^{-3} for the plasma density. It would then give 400s for an anomalous resistivity of $\eta = 10^{-7}$ and $4.\,10^5$s for a classical resistivity value of 10^{-13}. As concerns the amount of magnetic energy released, a value of order 10^{29} ergs (taking a loop length $L \simeq 10^8$ m) is obtained when one assume that it is independent of the resistivity. We then get flux rates of $8.\,10^7$ and $8.\,10^4$ erg/cm^{-2} s^{-1} for the anomalous and classical resistivities values respectively. As the observed heating flux in active regions is of order 10^7 erg/cm $^{-2}$/s, we can conclude that an anomalous resistivity with $\eta \sim 10^{-8}$ is required to explain the coronal heating in terms of reconnection associated with development of MHD kink instabilities in loops. The same conclusion also holds to account for a time scales of order minutes observed in flares. These simple estimates are based on a single loop event and do not take into account a large coronal region with many loops. Moreover, we have not considered the build up of the twist due to the photosperic flow. However, we believe that our results are useful to understand the role of reconnection in

coronal dynamics. A detailed discussion on the ability for kink instabilities to explain the observational features of transient brightening loops has been made by Arber et al. (1999).

It would be worth trying to extend the calculations presented in this paper to various different initial magnetic equilibria. Indeed, it has been shown that the form of the current concentration and the efficiency of the energy dissipation depend on the equilibrium parameters like the twist profile (Lionello et al. 1998a). Finally, one should note that recent simulations of a curved loop confined by an overlaying arcade show that the field lines of the loop reconnect with the arcade, resulting in a final state with two almost untwisted flux tubes (Amari & Luciani 1999). Therefore, the loop curvature effect is certainly not negligible. However, similarities in the current layer structure lead us to conclude that our results are a useful guideline in the understanding of the essential dymamics.

Acknowledgements. The numerical calculations were performed on the CRAY C98 at I.D.R.I.S., Orsay (France). The author thanks Jean Heyvaerts for fruitful discussions, and Thibaut Lery for careful reading of the manuscript. The author would like to thank Klaus Galsgaard for fruitful comments that helped improve the content of the paper.

References

Amari T., Luciani J.F., 1999, ApJ 515, L81
Arber T.D., Longbottom A.W., Van der Linden R.A.M., 1999, ApJ 517, 990
Aydemir A.Y., 1987, Phys. Fluids B2 (9), 2135
Baty H., Luciani J.F., Bussac M.N., 1991, Nuclear Fusion 31, 2055
Baty H., Heyvaerts J., 1996, A&A 308, 935
Baty H., 1997, A&A 318. 621
Baty H., Einaudi G., Lionello G., Velli M., 1998 A&A 333, 313
Beaufumé P., Coppi B., Golub L., 1992 ApJ 393, 396
Biskamp D., Welter H., 1980, Phys. Rev. Lett. 44, 1069
Biskamp D., 1993, Nonlinear Magnetohydrodynamics, Cambridge University Press, Cambridge.
Einaudi G., Van Hoven G., 1983, Solar Phys. 99, 163
Einaudi G., Lionello R., Velli M., 1997, Adv. Space Res. 19, 1875
Galsgaard K., Nordlund A., 1996, JGR, 101, 13445.
Galsgaard K., Nordlund A., 1997, JGR, 102,219.
Giovanelli R.G., 1947, MNRAS 107,338
Hood A.W., Priest E.R., 1979, Sol. Phys., 64, 303
Kadomtsev B.B, 1975 Sov. J. Plasma Phys. 1, 389
Lerbinger K., Luciani, 1991, J. Comput. Phys. 97, 444
Lionello R., Velli M., Einaudi. G., Mikic Z., 1998a ApJ 494, 840
Lionello R., Schnack D.D., Einaudi G., Velli M., 1998b Phys. Plasmas 10, 3722
Longcope D.W., Strauss H.R., 1994, ApJ 437, 851
Mikic Z., Schnack D.D., Van Hoven G., 1990, ApJ 437,851
Ng C.S., Bhattacharjee A., 1998, Phys. Plasmas 11, 4028
Park W., Monticello D.A., White R.B., 1984, Phys. Fluids 27, 137
Parker E.N., 1963, ApJs 77, 8
Parker E.N., 1972, ApJ 174, 499
Petschek H.E., 1964, in: Hess W.N. (ed.). AAS-NASA Symposium on Physics of Solar Flares (NASA SP-50), NASA, WAshington DC, p.425
Priest E.R., 1990, E.R. Priest and V Krishan (eds.), Basic Plasma Processes on the Sun, 271
Priest E.R., 1997, Phys. Plasmas 4, 1945
Raadu M.A., 1972, Solar Phys. 22, 425
Rickard G.J., Craig I.J.D., 1993, Phys. Fluids B5 (3), 956
Rosner R., Golub L., Coppi B., Vaiana G.S., 1978, ApJ 326, 418
Sweet P.A., 1958, in: Lehnert B. (ed.), IAU Symp. 6, Electromagnetic Phenomena in Cosmical Physics. Cambridge University Press, Cambridge, p.123
Tsuneta et al., 1991, Sol. Phys, 136, 37
Tsuneta S., 1996, ApJ 456, L63
Velli M., Einaudi G., Hood A.W., 1990, ApJ 350, 428
Velli M., Lionello R., Einaudi. G., 1997, Sol. Phys. 172, 257
Yoshida T., Tsuneta S., 1996, ApJ 459, 342